

EFFECT OF PLANAR DIELECTRIC INTERFACES ON FLUORESCENCE EMISSION AND DETECTION

Evanescent Excitation with High-Aperture Collection

THOMAS P. BURGHARDT

Cardiovascular Research Institute, University of California at San Francisco, San Francisco, California 94143

NANCY L. THOMPSON

Department of Chemistry, Stanford University, Stanford, California 94305

ABSTRACT We consider the effect of planar dielectric interfaces (e.g., solid/liquid) on the fluorescence emission of nearby probes. First, we derive an integral expression for the electric field radiated by an oscillating electric dipole when it is close to a dielectric interface. The electric field depends on the refractive indices of the interface, the orientation of the dipole, the distance from the dipole to the interface, and the position of observation. We numerically calculate the electric field intensity for a dipole on an interface, as a function of observation position. These results are applicable to fluorescent molecules excited by the evanescent field of a totally internally reflected laser beam and thus very close to a solid/liquid interface. Next, we derive an integral expression for the electric field radiated when a second dielectric interface is also close to the fluorescent molecule. We numerically calculate this intensity as observed through the second interface. These results are useful when the fluorescence is collected by a high-aperture microscope objective. Finally, we define and calculate a "dichroic factor," which describes the efficiency of collection, in the two-interface system, of polarized fluorescence. The limit when the first interface is removed is applicable for any high-aperture collection of polarized or unpolarized fluorescence. The limit when the second interface is removed has application in the collection of fluorescence with any aperture from molecules close to a dielectric interface. The results of this paper are required for the interpretation of order parameter measurements on fluorescent probes in supported phospholipid monolayers (Thompson, N. L., H. M. McConnell, and T. P. Burghardt, 1984, *Biophys. J.*, 46:739-747).

INTRODUCTION

An integral part of biophysical experiments that employ the dipolar nature of fluorescent molecules is an understanding of the propagation direction and polarization of the emitted fluorescence and of the efficiency of collection of the fluorescence. We consider in this paper the effect of planar dielectric interfaces (e.g., solid/liquid) on fluorescence emission and detection. The problem is generalized to include high-aperture collection of polarized fluorescence.

In the accompanying work (Thompson et al., 1984), we measure polarized fluorescence from probes attached to phospholipids in monolayers that are supported at the interface of an alkylated glass slide and solution. The probes are only a few angstroms from the supporting glass slide, so that the emitted field is strongly affected by the interface. This occurs for all fluorescent molecules excited with total internal reflection (for a recent review, see Axelrod et al., 1984). In addition, in the accompanying work, we make use of a high-aperture microscope objective

to collect light from a large solid angle. High-aperture objectives are particularly useful for measuring linear absorption dichroism, as detected by fluorescence (e.g., Burghardt et al., 1983) or by fluorescence correlation spectroscopy (Thompson and Axelrod, 1983).

The emission of a probe near an interface, as observed far from the molecule and the interface (the "far" or "asymptotic" field), has been calculated for some dipole orientations and in some regions (Carniglia et al., 1972; Lukosz and Kunz, 1977; Drexhage, 1974). In this paper, we calculate the emitted electric field of a dipole near an interface, for all dipole orientations and at all observation points. Then we calculate the emitted field from a dipole between two dielectric interfaces. We also calculate the effect of a high-aperture microscope lens on the polarization of the emitted field (Richards and Wolf, 1959; Axelrod, 1979) after the field has been transmitted through an interface. Combining the calculations of the emitted field and the effect of the lens on the polarization, we define factors multiplying the Cartesian components of the oscillating dipole moment that account for the net efficiency of

collection of emission from each component for this optical geometry. We make use of them in the accompanying paper for the interpretation of our data. In the limit of moving one interface to infinity, our calculations are applicable to the high-aperture collection of fluorescence from molecules in solution and are thus a generalization of the theory of Axelrod (1979).

OVERVIEW

The electric and magnetic fields radiated from an oscillating electric dipole have long been known in classical physics as the lowest order term in the expansion of the retarded vector potential (e.g., Jackson, 1975). The vector potential, A , for a dipole is a spherical wave and the electric and magnetic fields, E and B , are known (from A) in closed form at all points outside the source.

If an oscillating electric dipole is near a planar interface of conducting or dielectric materials, the radiated fields do not assume simple forms. Historically, the "dipole near a plane" problem has been approached by two methods. In the first method, a nearby conducting plane is replaced with an image (oscillating) dipole; the total fields are the superposition of fields from both dipoles (Kuhn, 1970; Morawitz, 1969). Another approach is to write the vector potential A (and thus the fields E and B) as an integral over plane waves. In this formalism, the effect of a planar interface is calculated from the sum of each plane wave as reflected or refracted at the interface. The plane wave expansion method is preferred because it clearly separates the fields into propagating transverse plane waves and waves that have longitudinal components ("evanescent" waves). It is the evanescent components that, in the absence of the interface, would normally not be observed at large distances from the dipole, but in the presence of the interface are converted into propagating, transverse plane waves. We begin our calculation by introducing the plane wave expansion of the electric field of an isolated, oscillating electric dipole.

EMISSION OF A DIPOLE AS AN INTEGRAL OVER PLANE WAVES

The vector potential of a dipole oscillating with angular frequency ω , located at the origin, is (Jackson, 1975):

$$A = (-ik/r_p) \hat{a} |a| \exp(ikr_p - i\omega t), \quad (1)$$

where r_p is the radial distance from the origin of the observation point, \hat{a} is the unit dipole moment, and $|a|$ is its magnitude, k is the wave number such that $k = \omega/v$, and v is the speed of light in the medium. The plane wave representation of A has been shown previously to be (Brekhovskikh, 1960):

$$A = -i(k^2 \hat{a} |a| / 2\pi) \int_{\Omega_z} d\Omega \exp(ik \cdot r_p - i\omega t), \quad (2)$$

where θ, ϕ are the spherical polar coordinates of the wave vector k such that $k = k(\sin \theta \cos \phi, \sin \theta \sin \phi, \cos \theta)$, and θ_p, ϕ_p are the spherical polar coordinates of the observation point r_p such that $r_p = r_p(\sin \theta_p \cos \phi_p, \sin \theta_p \sin \phi_p, \cos \theta_p)$. The paths of integration in Eq. 2 for $z_p \geq 0$ or $z_p \leq 0$ (where $z_p = r_p \cos \theta_p$), respectively, are Ω_z , where $\int_{\Omega_z} d\Omega = \int_0^{2\pi} d\phi \int_{C_z} \sin \theta d\theta$, and the paths of integration C_z in the complex θ plane are shown in Fig. 1. The electric field associated with this vector potential, given by $\nabla \times (\nabla \times A)/k$, where ∇ is the gradient operator, is:

$$E = -(ik^3 |a| / 2\pi) \int_{\Omega_z} d\Omega [k(k \cdot \hat{a}) - \hat{a}] \exp(ik \cdot r_p), \quad (3)$$

where we have suppressed the time-dependent factor $\exp(-i\omega t)$. Thus, both the vector potential and the electric field are infinite sums of plane waves with complex wave vectors k having different values of θ and ϕ , but equal magnitude k . This expression is also known in closed form (see Jackson, 1975).

The time-averaged electric field power per unit solid observation angle (Ω_p) is given by (apart from a multiplicative factor):

$$dP/d\Omega_p = (kr_p)^2 E \cdot E^*. \quad (4)$$

Fig. 2 shows (for later comparison) $dP/d\Omega_p$ calculated for a dipole pointed along the z axis, for radial distances $kr_p = 5$, and $kr_p \geq 20$ and for angles $\phi_p = 0^\circ$ and $\theta_p = 0$ to 180° . As $kr_p \rightarrow \infty$, $dP/d\Omega_p$ is proportional to $\sin^2 \theta_p$. When kr_p is finite, the field is slightly distorted from this asymptotic form because of contributions from evanescent waves.

EMISSION OF A DIPOLE NEAR A DIELECTRIC INTERFACE

We consider the emission field of a dipole located near the planar interface of two dielectrics with refractive indices n_1 and n_3 , as shown in Fig. 3. Frame F is defined so that the dipole is at the origin and the dielectric interface, referred to as the 1,3 interface, is at $z_p = -d_3$. (The subscript p is used to denote an observation point; a nonsubscripted variable describes a plane wave component inside the

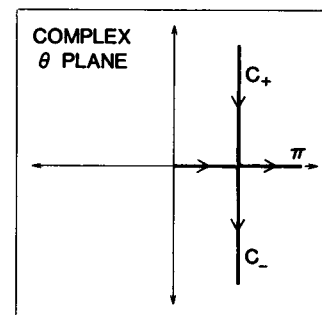


FIGURE 1 Paths of integration C_z in the complex θ plane for the plane wave representation of the vector potential A .

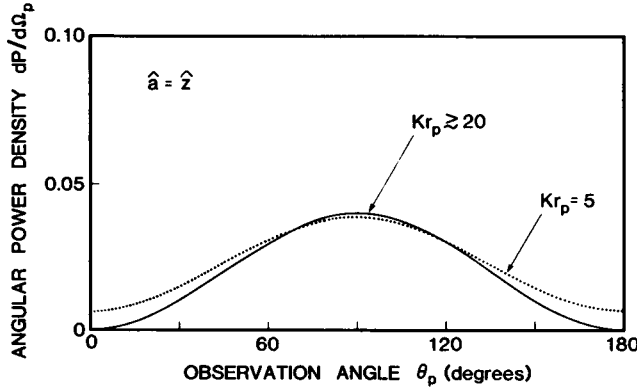


FIGURE 2 Electric field angular power density of an oscillating electric dipole in a homogeneous medium. Far from the dipole ($Kr_p \geq 20$), the power density is approximately equal to $\sin^2 \theta_p$; near the dipole (e.g., $Kr_p = 5$), the distribution has a different shape, and does not equal zero at $\theta_p = 0^\circ$ and 180° . The power density is plotted in arbitrary units; however, the units of Figs. 2, 4, and 5 are equivalent.

integral of Eq. 3.) In the $z_p > 0$ region, the field is a superposition of plane waves emitted from the oscillating dipole into the $z_p > 0$ half-space and those emitted into the $z_p < 0$ half-space but undergoing reflection at the interface and propagating back into the $z_p > 0$ half-space. In the $z_p < -d_3$ half-space (inside the dielectric with refractive index n_3), the field is the sum of plane waves propagating into the $z_p < 0$ half-space that are refracted at the interface.

The reflected and refracted fields for a given plane wave component are constructed using a coordinate frame F' located on the 1,3 interface with the z' axis pointing into the n_3 medium as shown in Fig. 3. The F' frame is a translation and a rotation from F such that an arbitrary plane wave with wave vector \mathbf{k} propagates in the $x'z'$ plane and intersects the interface at the origin of F' (each plane wave component has a different frame F'). The transformation of a vector from F to F' is a function of the azimuthal and polar angles of \mathbf{k} and is given by:

$$\begin{pmatrix} x_p' \\ y_p' \\ z_p' \end{pmatrix} = \begin{pmatrix} \cos \phi & \sin \phi & 0 \\ \sin \phi & -\cos \phi & 0 \\ 0 & 0 & -1 \end{pmatrix} \begin{pmatrix} x_p - x_0' \\ y_p - y_0' \\ z_p + d_3 \end{pmatrix}, \quad (5)$$

where $(x_0', y_0') = -d_3 \tan \theta (\cos \phi, \sin \phi)$ are translation distances along the x and y axes from the origin of F to the origin of F' . In F' , the reflected and transmitted fields, $\mathbf{E}_r^{13'}$ and $\mathbf{E}_t^{13'}$ are (Born and Wolf, 1980):

$$\begin{aligned} \mathbf{E}_r^{13'} &= (-r_1^{13} A_1^{13} \cos \theta_r', r_1^{13} A_1^{13}, r_1^{13} A_1^{13} \sin \theta_r') \exp(i\mathbf{k}_r' \cdot \mathbf{r}_p'); \\ \mathbf{E}_t^{13'} &= (-t_1^{13} A_1^{13} \cos \theta_t', t_1^{13} A_1^{13}, t_1^{13} A_1^{13} \sin \theta_t') \exp(i\mathbf{k}_t' \cdot \mathbf{r}_p'); \\ A_1^{13} &= (a_x \cos \theta \cos \phi + a_y \cos \theta \sin \phi + a_z \sin \theta) \\ &\quad \cdot \exp(-ikd_3/\cos \theta); \\ A_1^{13} &= (-a_x \sin \phi + a_y \cos \phi) \exp(-ikd_3/\cos \theta), \end{aligned} \quad (6)$$

where r^{13} and t^{13} are Fresnel coefficients, A^{13} are components of the complex amplitude of the incident plane wave, θ_r' and θ_t' are the angles of reflection and transmission of a plane wave incident on the 1,3 interface at $\pi - \theta$ (shown in Fig. 3), and \mathbf{k}_r' and \mathbf{k}_t' are the reflected and transmitted wave vectors in F' given by $\mathbf{k}_r' = k(\sin \theta_r', 0, \cos \theta_r')$ and $\mathbf{k}_t' = k_3(\sin \theta_t', 0, \cos \theta_t')$, where $k_3 = (n_3/n_1)k$. Transforming the plane wave fields of Eq. 6 back to the lab frame F and integrating over \mathbf{k} we arrive at expressions for the electric fields in the half-spaces $z_p > 0$ (index n_1) and $z_p < -d_3$ (index n_3).

It is convenient to describe the electric fields in a coordinate frame with its origin on the 1,3 interface. To do this, we define a coordinate $\mathbf{r}_{3,p} = (x_p, y_p, z_p + d_3)$. For $z_{3,p} > d_3$, we integrate over unperturbed and reflected plane waves, so that:

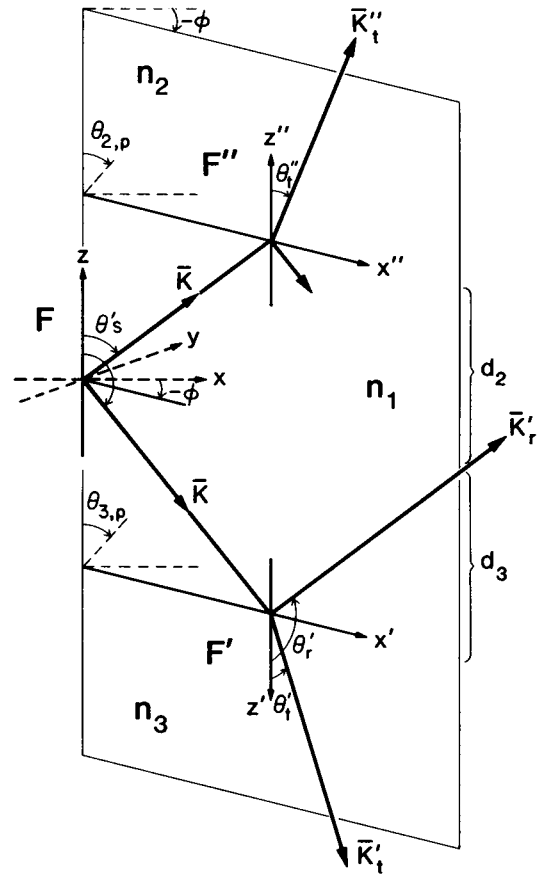


FIGURE 3 Coordinate frames. Frame $F(x, y, z)$ is defined so that the dipole is at its origin and z is perpendicular to the parallel planar dielectric interfaces. Each plane wave component emitted by the dipole is described by a wave vector $\mathbf{k}(\theta, \phi)$ in frame F . For the single-interface problem, frame $F'(x', y', z')$ is introduced, which has its origin at the point of intersection of a single plane wave component and the interface. The plane wave component travels in the $x'z'$ plane, and z' is parallel to z . Each plane wave component, with its \mathbf{k} vector, defines a different frame F' . The wave vectors of the reflected and refracted plane waves in the F' frame are given by $\mathbf{k}_r'(\theta_r')$ and $\mathbf{k}_t'(\theta_t')$. For the double-interface problem, a frame F'' analogous to F' is defined with origin at $z = d_2$.

$z_{3,p} \geq d_3$:

$$\mathbf{E} = -(ik^3 |\mathbf{a}|/2\pi) \int_{\Omega_s} d\Omega [\mathbf{k}(\mathbf{k} \cdot \hat{\mathbf{a}}) - \hat{\mathbf{a}} + \mathcal{E}_t^{13} \exp(2ikd_3 \cos \theta)] \cdot \exp(i\mathbf{k} \cdot \mathbf{r}_{3,p} - ikd_3 \cos \theta), \quad (7)$$

where (referring to Eq. 6):

$$\begin{aligned} (\mathcal{E}_t^{13})_{x,y} &= a_{x,y} [r_1^{13} \cos^2 \theta (\cos^2 \phi, \sin^2 \phi) - r_1^{13} (\sin^2 \phi, \cos^2 \phi)] \\ &+ a_{y,x} (r_1^{13} \cos^2 \theta + r_1^{13}) \sin \phi \cos \phi \\ &+ a_z r_1^{13} \sin \theta \cos \theta (\cos \phi, \sin \phi); \\ \mathcal{E}_{t,z}^{13} &= -a_x r_1^{13} \sin \theta \cos \theta \cos \phi \\ &- a_y r_1^{13} \sin \theta \cos \theta \sin \phi - a_z r_1^{13} \sin^2 \theta. \end{aligned} \quad (8)$$

For the region $z_{3,p} < 0$, we integrate over all refracted waves, so that:

$z_{3,p} \leq 0$:

$$\mathbf{E} = -(ik^3 |\mathbf{a}|/2\pi) \int_{\Omega_s} d\Omega \mathcal{E}_t^{13} \exp(i\mathbf{k}_t^{13} \cdot \mathbf{r}_{3,p} + ikd_3 \cos \theta), \quad (9)$$

where $\mathbf{k}_t^{13} = k_3(\sin \theta'_i \cos \phi, \sin \theta'_i \sin \phi, -\cos \theta'_i)$ and the transmitted amplitude \mathcal{E}_t^{13} is:

$$\begin{aligned} (\mathcal{E}_t^{13})_{x,y} &= a_{x,y} [-t_1^{13} \cos \theta \cos \theta'_i (\cos^2 \phi, \sin^2 \phi) - t_1^{13} (\sin^2 \phi, \cos^2 \phi)] + a_{y,x} (-t_1^{13} \cos \theta \cos \theta'_i \\ &+ t_1^{13}) \sin \phi \cos \phi \\ &- a_z t_1^{13} \sin \theta \cos \theta'_i (\cos \phi, \sin \phi); \\ \mathcal{E}_{t,z}^{13} &= a_x (-t_1^{13} \sin \theta'_i \cos \theta \cos \phi) \\ &+ a_y (-t_1^{13} \sin \theta'_i \cos \theta \sin \phi) \\ &+ a_z (-t_1^{13} \sin \theta \sin \theta'_i). \end{aligned} \quad (10)$$

The fields in Eqs. 7 and 8 and Eqs. 9 and 10 can be calculated numerically, and are applicable for any values of n_1 and n_3 , and at all points $z_{3,p} \leq 0$ or $z_{3,p} \geq d_3$. The angular power density as observed in the xz plane is plotted in Fig. 4 for a dipole on the interface ($d_3 = 0$); $n_1 = 1.334$ (water) and $n_3 = 1.5$ (glass); $kr_{3,p} = 5, 20$ and ∞ ; and for dipoles $\hat{\mathbf{a}}$ that are in the plane of, and perpendicular to, the interface. As shown, the angular power density for $\hat{\mathbf{a}} = \hat{\mathbf{z}}$ and $kr_{3,p} = 5$ and 20 shows a discontinuity at the interface where $\theta_{3,p} = 90^\circ$ (see Fig. 4a). This is from the discontinuity of the normal component of the electric field at the interface. The normal component of \mathbf{E} is the predominant contributor to the power density for a dipole oriented normal to the interface. When the dipole is oriented in the plane of the interface ($\hat{\mathbf{a}} = \hat{\mathbf{x}}$ or $\hat{\mathbf{a}} = \hat{\mathbf{y}}$) and $kr_{3,p} = 5$ and 20 , the predominant polarization of the electric field contributing to the angular power density is tangential to the

interface, so that the power density appears continuous across the interface (see Fig. 4, b and c). The asymptotic curves ($kr_{3,p} \rightarrow \infty$) agree with previously published curves for the case of $\hat{\mathbf{a}} = \hat{\mathbf{z}}$ (Lukosz and Kunz, 1977) and for $\hat{\mathbf{a}} = \hat{\mathbf{y}}$ (Carniglia et al., 1972). We note that on the higher refractive index side of observation, light is emitted into observation angles in the angular region $90^\circ \leq \theta_{3,p} \leq 180^\circ - \sin^{-1}(n_1/n_3) = 117.2^\circ$, which would not occur for a dipole located far from the interface in the lower refractive index region. This is from evanescent waves emitted by the dipole that are changed by the interface into propagating plane waves, as has been observed experimentally (Carniglia et al., 1972).

EMISSION OF A DIPOLE BETWEEN TWO INTERFACES

We now place the dipole between two dielectric interfaces. The second interface may represent a nearby microscope objective. The new interface reflects and refracts incident plane waves. This alters the effective aperture of any objective. The interface also perturbs the emitted evanescent waves such that some of them become transverse propagating waves. This effect is strongly dependent on the distance from the dipole to the second interface.

The geometry of the two-interface system is shown in Fig. 3. The new interface between dielectrics of refractive indices n_1 and n_2 is positioned at $z = d_2$. Coordinate frame F'' , analogous to frame F' , is defined such that a plane wave with wave vector \mathbf{k} is incident in the $x''z''$ plane and intersects the interface at the origin of F'' . The transformation of a vector from F to F'' is a function of the angles of \mathbf{k} and is given by:

$$\begin{pmatrix} x_p'' \\ y_p'' \\ z_p'' \end{pmatrix} = \begin{pmatrix} \cos \phi & -\sin \phi & 0 \\ \sin \phi & \cos \phi & 0 \\ 0 & 0 & 1 \end{pmatrix} \begin{pmatrix} x_p - x_0'' \\ y_p - y_0'' \\ z_p - d_2 \end{pmatrix}, \quad (11)$$

where $(x_0'', y_0'') = d_2 \tan \theta (\cos \phi, \sin \phi)$ are translation distances along the x and y axes from the origin of F to the origin of F'' . In F'' , the transmitted plane waves have electric fields $\mathbf{E}_t^{12''}$, given by:

$$\begin{aligned} \mathbf{E}_t^{12''} &= [-t_1^{12} A_1^{12} \cos \theta'_i, t_1^{12} A_1^{12}, t_1^{12} A_1^{12} \sin \theta'_i] \exp(i\mathbf{k}_t'' \cdot \mathbf{r}_p''); \\ A_1^{12} &= \{[a_x \cos \phi + a_y \sin \phi] \cos \theta [1 - r_1^{13} \exp(2ikd_3 \cos \theta)] \\ &- a_z \sin \theta [1 + r_1^{13} \exp(2ikd_3 \cos \theta)]\} \exp(ikd_2/\cos \theta); \\ A_1^{12} &= (a_x \sin \phi - a_y \cos \phi) \\ &\cdot [1 + r_1^{13} \exp(2ikd_3 \cos \theta)] \exp(ikd_2/\cos \theta), \end{aligned} \quad (12)$$

where t_1^{12} are Fresnel coefficients for the 1,2 interface θ'_i is the angle of refraction of a plane wave incident on the 1,2 interface at angle θ , $\mathbf{k}_t'' = k_2(\sin \theta'_i, 0, \cos \theta'_i)$ is the transmitted wave vector, $k_2 = (n_2/n_1)k$, and A_1^{12} are components of the complex amplitude of the incident plane waves that arise both from direct emission of the dipole and emission followed by reflection at the 1,3 interface.

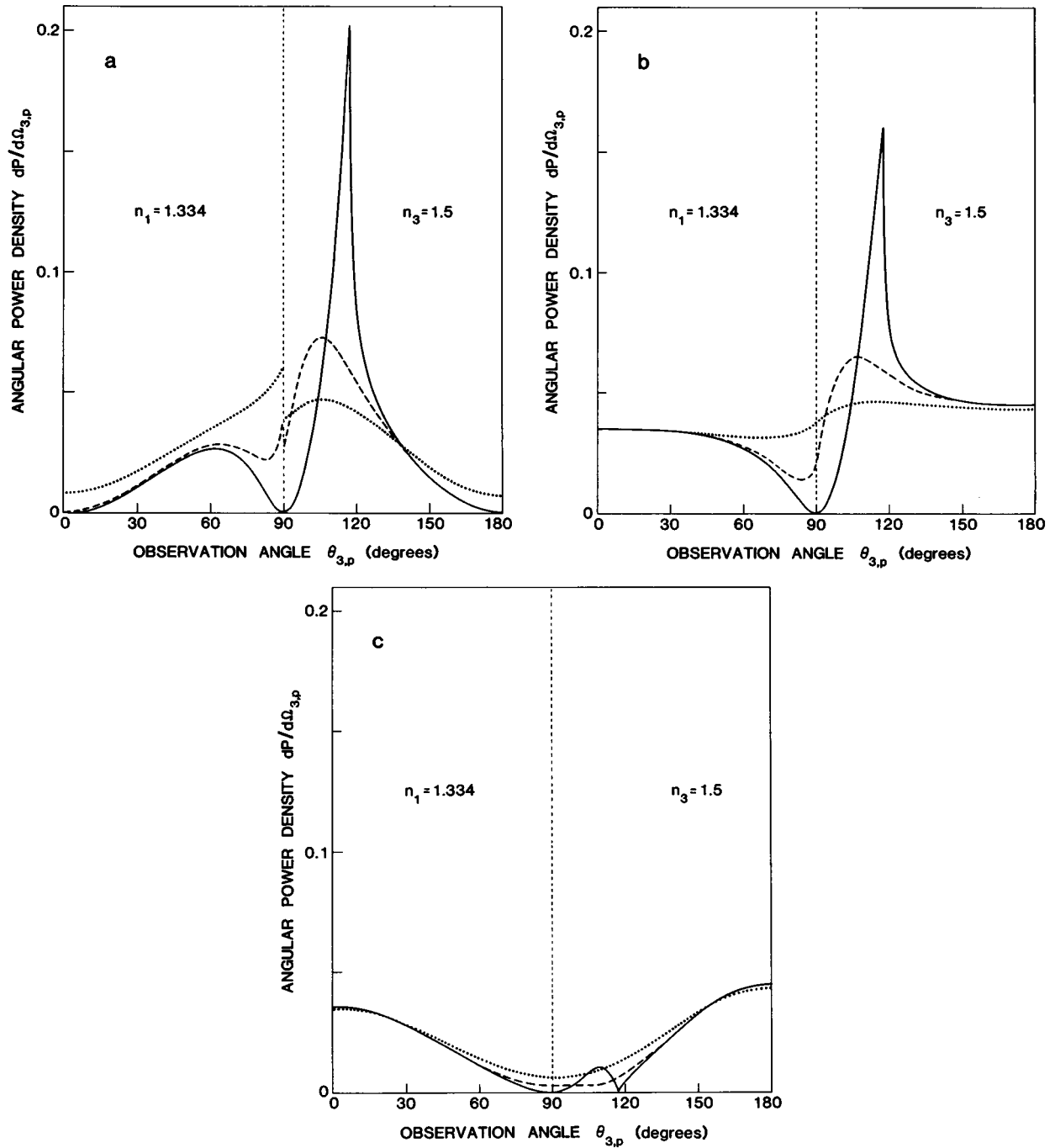


FIGURE 4 Electric field angular power density of an oscillating electric dipole on a dielectric interface. The angular density is shown for a dipole along \hat{z} , \hat{y} , and \hat{x} (a, b, and c), as observed for $r_{3,p} = 5$ (\cdots), $r_{3,p} = 20$ ($---$), and $r_{3,p} \rightarrow \infty$ ($—$), $\theta_{3,p} = 0^\circ$ to 180° , and $\phi_{3,p} = 0^\circ$. The refractive indices are $n_1 = 1.334$ (water) and $n_3 = 1.5$ (glass), and distance d_3 is zero.

There are contributions to the electric field transmitted through the 1,2 interface from plane waves undergoing multiple reflections between the interfaces. The correction to the transmitted field from this effect is obtained by making the replacement $t^{12} \rightarrow q^{12} \equiv t^{12}/[1 - r^{12}r^{13} \exp\{2ik(d_2 + d_3)\cos\theta\}]$. This result is a simple alteration of an expression derived by Born and Wolf (1980).

It is convenient to describe the transmitted field in terms

of a coordinate frame fixed on the 1,2 interface. To do this, we define a coordinate $\mathbf{r}_{2,p} = (x_p, y_p, z_p - d_2)$, so that

$z_{2,p} \geq 0$:

$$\mathbf{E} = -(ik^3|\mathbf{a}|/2\pi) \int_{\Omega_2} d\Omega \mathcal{E}_i^{12} \cdot \exp(ik_i^{12} \cdot \mathbf{r}_{2,p} + ikd_2 \cos\theta), \quad (13)$$

where $\mathbf{k}_i^{12} = k_2(\sin \theta_i' \cos \phi, \sin \theta_i' \sin \phi, \cos \theta_i')$ and

$$\begin{aligned}
 (\mathcal{E}_i^{12})_{x,y} &= a_{x,y} \{ \cos \theta \cos \theta_i' (\cos^2 \phi, \sin^2 \phi) q_i^{12} \\
 &\quad [r_i^{13} \exp(2ikd_3 \cos \theta) - 1] - (\sin^2 \phi, \cos^2 \phi) q_i^{12} \\
 &\quad \cdot [1 + r_i^{13} \exp(2ikd_3 \cos \theta)] \} + a_{y,x} \{ \cos \theta \cos \theta_i' q_i^{12} \\
 &\quad [r_i^{13} \exp(2ikd_3 \cos \theta) - 1] \\
 &\quad + q_i^{12} [1 + r_i^{13} \exp(2ikd_3 \cos \theta)] \} \sin \phi \cos \phi \\
 &\quad + a_z \sin \theta \cos \theta_i' (\cos \phi, \sin \phi) q_i^{12} \\
 &\quad \cdot [1 + r_i^{13} \exp(2ikd_3 \cos \theta)]; \\
 \mathcal{E}_{i,z}^{12} &= a_x \cos \theta \sin \theta_i' \cos \phi q_i^{12} [1 - r_i^{13} \exp(2ikd_3 \cos \theta)] \\
 &\quad + a_y \cos \theta \sin \theta_i' \sin \phi q_i^{12} [1 - r_i^{13} \exp(2ikd_3 \cos \theta)] \\
 &\quad - a_z \sin \theta \sin \theta_i' q_i^{12} [1 + r_i^{13} \exp(2ikd_3 \cos \theta)]. \quad (14)
 \end{aligned}$$

The field in Eq. 13 can be calculated numerically and is applicable for any values of n_1 , n_2 , and n_3 , and at all points $\theta_{2,p} \leq 90^\circ$. The electric field angular power density as observed in the xz plane in the region $z_{2,p} \geq 0$ is plotted in Fig. 5 for $kd_3 = 0$, $kd_2 = 640$, $n_1 = 1.334$, $n_2 = n_3 = 1.5$, and with $kr_{2,p} \rightarrow \infty$, for dipoles in the plane of, and perpendicular to, the interfaces. Comparing Fig. 5 with Fig. 4, we see that the 1,2 interface appreciably alters the electric field power density distribution in space by focusing the power densities of Fig. 4 into a cone with a half-angle of approximately $\sin^{-1}(n_1/n_2) = 63^\circ$.

The magnitude of the power density rapidly oscillates as a function of $\theta_{2,p}$ when $\theta_{2,p}$ nears the critical angle of the 1,2 interface. This is from interference of the plane wave transmitted directly through the 1,2 interface with plane waves that undergo multiple reflections between the 1,2 and 1,3 interfaces and are then transmitted. This effect is dependent on the 1,2 and the 1,3 interfaces being flat and

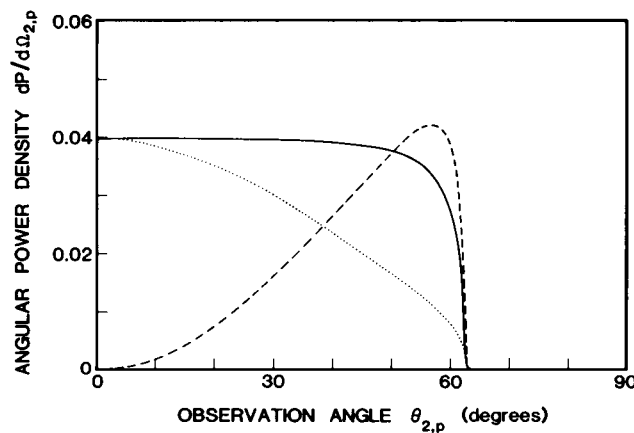


FIGURE 5 Electric field angular power density of an oscillating electric dipole between two dielectric interfaces as observed in a finite aperture. The refractive indices are $n_1 = 1.334$ (water) and $n_2 = n_3 = 1.5$ (glass); the dipole lies on one interface ($d_3 = 0$), which is a distance $d_2 = 640/k$ from the other interface (see Fig. 3). The finite aperture subtends 0.5° . Shown is the angular density observed far away from the dipole ($kr_p \rightarrow \infty$) in the n_2 medium, as a function of $\theta_{2,p} = \tan^{-1}[(z - d_2)/x]$, and at $\theta_{2,p} = 0^\circ$, with $\hat{a} = \hat{z}$ (---), $\hat{a} = \hat{y}$ (—), $\hat{a} = \hat{x}$ (···).

parallel. These rapid power density oscillations would not normally be observed because any real detector will subtend a solid angle over which the oscillations would be averaged. In Fig. 5 we have plotted the power density as observed in a finite aperture detector.

The effect of evanescent wave emission of the dipole is to emit energy in the n_2 medium where $\theta_{2,p} > 62.7^\circ$. This contribution to the power density is small for $kd_2 = 640$, as shown in Fig. 5. The evanescent wave contribution to the emitted power becomes significant when $kd_2 \lesssim 15$ (curve not shown).

THE EFFECT OF A LENS ON THE POLARIZATION OF LIGHT

The collection of a linearly polarized plane wave by a lens, originally treated by Richards and Wolf (1959), has found application in biophysics (Axelrod, 1979; Burghardt and Thompson, 1984). The calculation is based on the conservation of the angle α between the direction of the electric field and the meridional plane, and the refraction of the plane wave from the focal plane into a plane wave propagating along the optical axis. The optical path of a typical ray is shown in Fig. 6. Applying these rules to the dipolar emission of Eq. 13, we show that the electric field from a dipole at position \mathbf{u}_0 in the focal plane of the objective is:

$$\begin{aligned}
 e_{x,y} &= -iA \int_{S_0} d\Omega \{ (\mathcal{E}_i^{12})_{x,y} \\
 &\quad \cdot [\cos \theta_i' (\cos^2 \phi, \sin^2 \phi) + (\sin^2 \phi, \cos^2 \phi)] \\
 &\quad + (\mathcal{E}_i^{12})_{y,x} \sin \phi \cos \phi (\cos \theta_i' - 1) \\
 &\quad - \mathcal{E}_{i,z}^{12} \sin \theta_i' (\cos \phi, \sin \phi) \} \\
 &\quad \cdot \exp(-i\mathbf{k} \cdot \mathbf{u}_0 + ikd_2 \cos \theta + ik_0 z_{2,p}), \quad (15)
 \end{aligned}$$

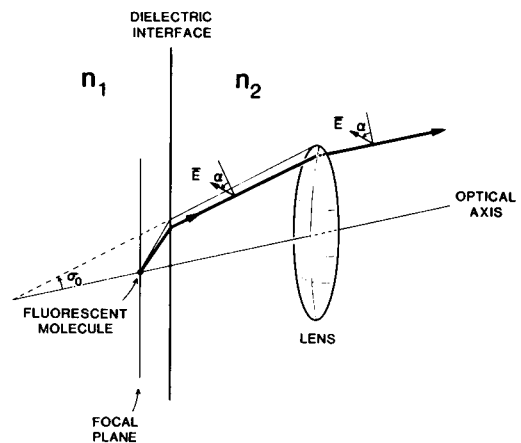


FIGURE 6 Collection of polarized light by a lens. A fluorescent molecule is in the focal plane of a lens. A plane wave component of its emitted field is refracted at an interface between refractive indices n_1 and n_2 . When the ray passes into the lens, the angle α between the electric field and the meridional plane is conserved. The collected ray is refracted by the lens and travels in image space along the optical axis. Aperture angle σ_0 is given by $\sin^{-1}(NA/n_2)$.

where A is an amplitude dependent on the composition of the lens, and \mathbf{k}_0 is the wave vector in the object space. The plane wave represented by $\exp(ik_0 z_{2,p})$ propagates along the z axis. The integration is along a complex path S_0 that includes propagating (real \mathbf{k}) and evanescent (complex \mathbf{k}) components that are admitted by the aperture of the lens.

Our calculation is greatly simplified by writing the integral in terms of the refraction angle θ'_i and neglecting contributions from complex transmitted waves. This is a legitimate approximation for the detected field because the detector is located far from the emitting dipole, where exponentially decaying field amplitudes are zero. From the relationship

$$\sin \theta \, d\theta \, d\phi = \frac{\cos \theta'_i}{\cos \theta} \sin \theta'_i \, d\theta'_i \, d\phi, \quad (16)$$

we write Eq. 15 in the form:

$$\begin{aligned} e_{x,y} = & -iA \int_0^{\sigma_0} \sin \theta'_i \, d\theta'_i (\cos \theta'_i / \cos \theta) \int_0^{2\pi} d\phi \\ & \cdot \{(\mathcal{E}_i^{12})_{x,y} [\cos \theta'_i (\cos^2 \phi, \sin^2 \phi) + (\sin^2 \phi, \cos^2 \phi)] \\ & + (\mathcal{E}_i^{12})_{y,x} \sin \phi \cos \phi (\cos \theta'_i - 1) \\ & - \mathcal{E}_{i,x}^{12} \sin \theta'_i (\cos \phi, \sin \phi)\} \\ & \cdot \exp(-i\mathbf{k}_i^2 \cdot \mathbf{u}_0 + ikd_2 \cos \theta + ik_0 z_{2,p}), \end{aligned} \quad (17)$$

where the integration over ϕ and θ'_i is on the real axis, σ_0 is the angle the lens aperture subtends in object space, as shown in Fig. 6, and functions of θ and θ'_i are written in terms of θ'_i using Snell's Law, $n_1 \sin \theta = n_2 \sin \theta'_i = n_3 \sin \theta'_i$.

For a population of independent molecules with different positions \mathbf{u}_0 in the plane of focus, the detected power polarized along x or y , which we call P_x or P_y , is the emitted field intensity integrated over all molecules, i.e., $\int d\mathbf{u}_0 \mathbf{E} \cdot \mathbf{E}^*$.

When the dimensions of the focal plane are large compared with the wavelength of light, the term $\int d\mathbf{u}_0 \exp\{-i\mathbf{u}_0 \cdot [\mathbf{k}(\theta, \phi) - \mathbf{k}(\theta', \phi')]\}$ in P_x or P_y is well approximated by $\delta[\mathbf{k}(\theta, \phi) - \mathbf{k}(\theta', \phi')]$, where δ is a Dirac delta function. The observed power is then given by:

$$\begin{aligned} P_{x,y} = & A^2 \int_0^{\sigma_0} \sin \theta'_i \, d\theta'_i \int_0^{2\pi} d\phi \\ & \cdot \{(\mathcal{E}_i^{12})_{x,y} [\cos \theta'_i (\cos^2 \phi, \sin^2 \phi) + (\sin^2 \phi, \cos^2 \phi)] \\ & + (\mathcal{E}_i^{12})_{y,x} \sin \phi \cos \phi (\cos \theta'_i - 1) \\ & - \mathcal{E}_{i,x}^{12} \sin \theta'_i (\cos \phi, \sin \phi)\} \\ & \cdot (\cos \theta'_i / \cos \theta) \exp(ikd_2 \cos \theta)^2. \end{aligned} \quad (18)$$

This expression can be written in the form

$$P_{x,y} = A^2 (K_a a_{x,y}^2 + K_b a_{y,x}^2 + K_a a_z^2), \quad (19)$$

where, after ϕ integration,

$$K_a = \int_0^{\sigma_0} \sin \theta'_i \, d\theta'_i \cos^2 \theta'_i \sin^2 \theta$$

$$|q|^2 [1 + r_1^3 \exp(2ikd_3 \cos \theta)] / \cos \theta|^2 \\ \exp[ikd_2 (\cos \theta - \cos^* \theta)];$$

$$\begin{aligned} K_b = & 1/4 \int_0^{\sigma_0} \sin \theta'_i \, d\theta'_i \cos^2 \theta'_i \\ & |\cos \theta q|^2 [1 - r_1^3 \exp(2ikd_3 \cos \theta)] \\ & - q_{\perp}^{12} [1 + r_1^3 \exp(2ikd_3 \cos \theta)] / \cos \theta|^2 \\ & \cdot \exp[ikd_2 (\cos \theta - \cos^* \theta)]; \end{aligned}$$

$$\begin{aligned} K_c = & 1/4 \int_0^{\sigma_0} \sin \theta'_i \, d\theta'_i (\cos^2 \theta'_i / |\cos \theta|^2) \\ & \cdot (3 |\cos \theta q|^2 [1 - r_1^3 \exp(2ikd_3 \cos \theta)]|^2 \\ & + 3 |q_{\perp}^{12} [1 + r_1^3 \exp(2ikd_3 \cos \theta)]|^2 \\ & + \{\cos \theta q\}^2 [1 - r_1^3 \exp(2ikd_3 \cos \theta)] \\ & \cdot \{q_{\perp}^{12} [1 + r_1^3 \exp(2ikd_3 \cos \theta)]\}^* \\ & + \{\cos \theta q\}^2 [1 - r_1^3 \exp(2ikd_3 \cos \theta)] \\ & \cdot \{q_{\perp}^{12} [1 + r_1^3 \exp(2ikd_3 \cos \theta)]\} \\ & \cdot \exp[ikd_2 (\cos \theta - \cos^* \theta)]. \end{aligned} \quad (20)$$

If the emitting dipole is located in the medium with refractive index n_3 (Fig. 3), then light emitted by the dipole transmits the 1,3 and 1,2 interfaces before collection by the lens. To treat this problem, we define (as before) d_3 and d_2 as the distances from the dipole to the 1,3 and 1,2 interfaces (distance $d_2 - d_3$ is the distance between the interfaces). We then follow a procedure analogous to the one above and show that the new factors K_a , K_b , and K_c have the form of those in Eq. 20, with $r^{13} \exp(ik_3 d_3 \cos \theta)$ replacing $1 \pm r^{13} \exp(2ikd_3 \cos \theta)$ and $kd_2 \cos \theta'_i$ replacing $kd_2 \cos \theta$.

Factors K_a , K_b , and K_c reduce to those derived by Axelrod (1979) when $n_1 = n_2 = n_3$. These factors summarize the collection efficiencies for components of an emission dipole after taking into account both interfaces and depolarization by high-aperture optics. Use of these factors in less general form has been demonstrated in calculations of polarization of fluorescence from ordered systems (Burghardt, 1984). We use them now to calculate an optical correction in application to the dichroism of fluorescence technique discussed in the accompanying paper.

DICHOIC FACTOR γ : APPLICATION TO LINEAR DICHOISM OF FLUORESCENCE

The total collected fluorescence is proportional to $P_0 = P_x + P_y$ which, from Eq. 19, is equal to:

$$P_0 = A^2 (K_b + K_c) (1 - \gamma a_z^2), \quad (21)$$

where

$$\gamma = 1 - 2 K_a / (K_b + K_c). \quad (22)$$

Factor γ , which we call the "dichroic factor," ranges from 1 to $-\infty$. A positive (or negative) γ indicates that less (or

more) light is collected from an emission dipole oriented along the z axis (the optical axis in Fig. 6) than from one oriented in the xy plane. When $\gamma = 0$, the collected fluorescence is independent of the direction of the emission dipole.

A central assumption of the ideal dichroism of fluorescence experiment (see accompanying paper) is that $\gamma = 0$. This condition is achieved, in the absence of nearby interfaces, when the collection optics collect light from 2π steradians (Borejdo et al., 1982; Burghardt et al., 1983). In a nonideal system, such as we have considered here, γ is not zero. In Fig. 7, we have plotted γ vs. σ_0 , the lens aperture angle (see Fig. 6). Angle σ_0 equals $\sin^{-1}(\text{NA}/n_2)$, where NA is the numerical aperture of the objective. In Fig. 7a is shown γ when only the coverslip (1,2 interface) is present. These factors are applicable to the observation of polarized light (by oil immersion objectives) when the source is in a homogeneous medium. In Fig., 7b and c, are shown γ when both interfaces are present and the dipole is in the n_1 and n_3 medium, respectively. We have chosen several values of $n_1 < n_2 = n_3 = 1.5$ (glass), the dipoles to be on the 1,3 interface ($d_3 = 0$), and the 1,2 and 1,3 interfaces to be separated by 640 inverse wave numbers ($\approx 50 \mu\text{m}$). As shown, increasing σ_0 beyond the critical angle defined by $\theta_c = \sin^{-1} n_1/n_2$ does not decrease γ significantly since only evanescent waves emerge past θ_c in the n_2 region and they have been attenuated exponentially over the distance from the dipole to the 1,2 interface. This minimum value of γ is not zero, when $\sigma_0 = \theta_c$ because of the reflectivity of the 1,2 interface. Nondichroic collection optics ($\gamma = 0$) are achieved only when $n_1 = n_2 = n_3$ and $\sigma_0 = 90^\circ$ (Fig. 7a). Microscope objectives with these specifications are not commercially available. An alternative would be to employ nonimaging optics (Welford and Winston, 1978). We also note that for the conditions of the accompanying paper ($n_1 = 1.334$, $n_2 = n_3 = 1.5$, $kd_3 = 0$, $kd_2 = 640$, $\sigma_0 = 69.6^\circ$), γ is 0.1 for a dipole in the n_1 medium and γ is 0.44 for a dipole in the n_3 medium.

SUMMARY

The angular emission pattern of a system containing dipole oscillators can be used to deduce the orientation distribution of the dipole emitters. This is done in all order measurements employing fluorescence polarization or linear dichroism of fluorescence. Interpreting the ordered system's emission pattern to deduce the orientation of the dipole emitters requires that the shape of the emission pattern from a single dipole be known. In this paper, we have derived integral expressions for the electric field emitted by an oscillating electric dipole when the dipole is near a dielectric interface. Our two-interface system models the optical system used in the accompanying paper (Thompson et al., 1984) and is generally useful for any system wherein high-aperture collection optics are employed.

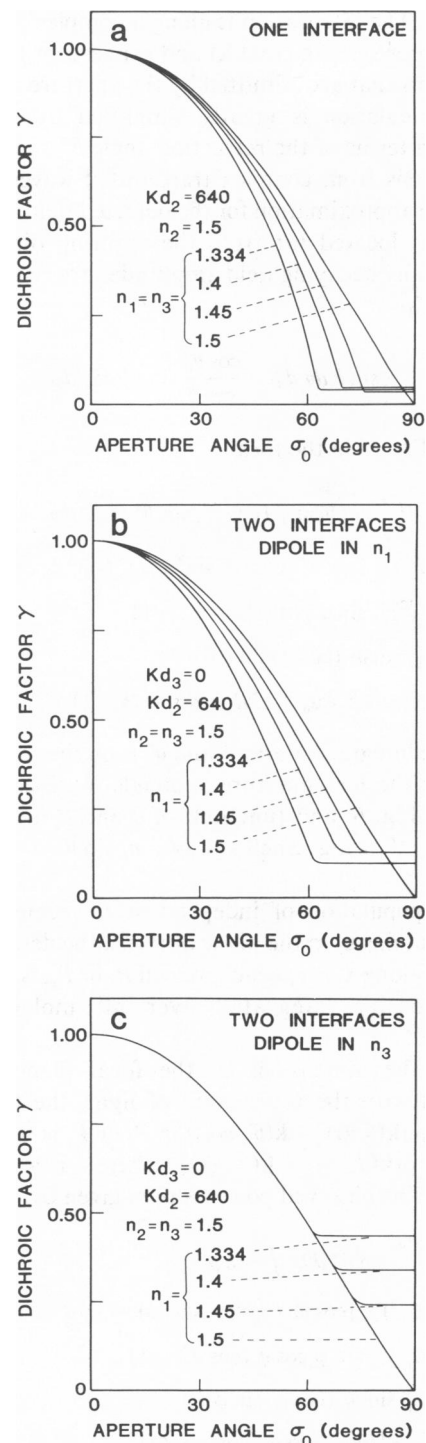


FIGURE 7 Dichroic factor γ as a function of aperture angle σ_0 . Shown are values of the factor γ calculated from Eqs. 22 and 20. Parameters are: (a) $kd_2 = 640$, $n_2 = 1.5$, $n_1 = n_3 = 1.334, 1.4, 1.45, 1.5$; (b) $kd_3 = 0$, $kd_2 = 640$, $n_2 = n_3 = 1.5$, $n_1 = 1.334, 1.4, 1.45, 1.5$ where the dipole is in medium of n_1 ; (c) same as b, except that the dipole is in medium n_3 .

This work was supported by American Heart Association Postdoctoral Fellowship 82 071 (to T. P. Burghardt) and by Damon Runyon-Walter Winchell Cancer Fund Postdoctoral Fellowship 593 (to N. L. Thompson), National Institutes of Health grant 5R01 AI13587 (to Harden McConnell of Stanford University), and U.S. Public Health Service grant HL-16683 (to Manuel F. Morales of the University of California, San Francisco).

Received for publication 3 February 1984 and in final form 13 July 1984.

REFERENCES

- Axelrod, D. 1979. Carboyanine dye orientation in red cell membrane studied by microscopic fluorescence polarization. *Biophys. J.* 26:557-574.
- Axelrod, D., T. P. Burghardt, and N. L. Thompson. 1984. Total internal reflection fluorescence. *Annu. Rev. Biophys. Bioeng.* 13:247-268.
- Borejdo, J., O. Assulin, T. Ando, and S. Putman. 1982. Cross-bridge orientation in skeletal muscle measured by linear dichroism of an extrinsic chromophore. *J. Mol. Biol.* 158:391-414.
- Born, M., and E. Wolf. 1980. Principles of Optics. Pergamon Press, New York. 36-261.
- Brekhovskikh, L. M. 1960. Waves in Layered Media. Academic Press, Inc., New York. 234-261.
- Burghardt, T. P. 1984. Model independent fluorescence polarization for measuring order in a biological assembly. *Biopolymers*. In press.
- Burghardt, T. P., T. Ando, and J. Borejdo. 1983. Evidence for cross-bridge order in contraction of glycerinated skeletal muscle. *Proc. Natl. Acad. Sci. USA*. 80:7515-7519.
- Burghardt, T. P., and N. L. Thompson. 1984. Evanescent intensity of a focused Gaussian light beam undergoing total internal reflection in a prism. *Opt. Eng.* 23:62-67.
- Carniglia, C. K., L. Mandel, and K. H. Drexhage. 1972. Absorption and emission of evanescent photons. *J. Opt. Soc. Am.* 12:479-486.
- Drexhage, K. H. 1974. Interaction of light with monomolecular dye layers. *Prog. Optics*. 12:163-232.
- Jackson, J. D. 1975. Classical Electrodynamics. John Wiley & Sons, New York. Second ed. 391-397.
- Kuhn, H. 1970. Classical aspects of energy transfer in molecular systems. *J. Chem. Phys.* 53:101-108.
- Lukosz, W., and R. E. Kunz. 1977. Light emission by magnetic and electric dipoles close to a plane dielectric interface. II. Radiation patterns of perpendicular oriented dipoles. *J. Opt. Soc. Am.* 67:1615-1619.
- Morawitz, H. 1969. Self-coupling of a two-level system by a mirror. *Phys. Rev.* 187:1792-1796.
- Richards, B., and E. Wolf. 1959. Electromagnetic diffraction in optical systems. II. Structure of the image field in an aplanatic system. *Proc. R. Soc. Edinb. Sect. (Math. Phys. Sci.) A* 253:358-379.
- Thompson, N. L., and D. Axelrod. 1983. Immunoglobulin surface-binding kinetics studied by total internal reflection with fluorescence correlation spectroscopy. *Biophys. J.* 43:103-114.
- Thompson, N. L., H. M. McConnell, and T. P. Burghardt. 1984. Order in supported phospholipid monolayers detected by the dichroism of fluorescence excited with polarized evanescent illumination. *Biophys. J.* 46:739-747.
- Welford, W. T., and R. Winston. 1978. The Optics of Nonimaging Concentrators: Light and Solar Energy. Academic Press, Inc., New York. 47-64.